A Numerical Investigation of Conductor Casing Installation Using Material Point Method

Mávyla Sandreya Correia Tenório[1], Jennifer Mikaella Ferreira Melo[1], Beatriz Ramos Barboza[1], Raniel Deivisson de Alcantara Albuquerque[2], João Paulo Lima Santos[1], Fábio Sawada Cutrim[3], Rafael Dias[3]

[1] *Laboratory of Scientific Computing and Visualization, Federal University of Alagoas*
Cidade Universitária, 57072-970, Alagoas, Brazil
mavyla.tenorio@lccv.ufal.br, jennifer.ferreira@lccv.ufal.br, beatriz@lccv.ufal.br, jpls@lccv.ufal.br
[2] *COPPE, Federal University of Rio de Janeiro*
Cidade Universitária, 21941-901, Rio de Janeiro, Brazil
raniel.albuquerque@coc.ufrj.br
[3] *Petrobras*
Edifício Senado. Rua Henrique Valadares, 20231-030, Rio de Janeiro, Brazil
fabiosawada@petrobras.com.br, rafael_dias@petrobras.com.br

Abstract. The initial phases of well drilling projects involve the crucial step of installing conductor casing, which can be achieved through various methods, including conductor driving. Given the often-challenging environmental conditions, conducting experimental analyses of drilling parameters becomes impractical. Consequently, numerical modeling emerges as a feasible and reliable alternative for process control. In this study, the open-source software ANURA 3D was adopted, which utilizes the Material Point Method (MPM) in its solutions. Therefore, this research aims to explore the impact of some numerical parameters associated with computational modeling on problem solution. For this purpose, a two-dimensional axisymmetric computational model of self-weight penetration was employed. In this work, the influence of material point specification and time step size was analyzed. Increasing material point specification provided results for vertical displacement and tension distribution; however, beyond a certain point, the results do not show any significant differences, only an increase in computational costs. It was also observed that, for the time step sizes considered in this analysis, no significant differences could be noted, despite minor time step increase accuracy of results.

Keywords: MPM; Drilling; Conductor Casing.

1 Introduction

Advancements in computer technology have made numerical simulation crucial across various engineering fields. One of the reasons for this is that computer modeling offers the possibility of optimizing and investigating processes, such as offshore oil well drilling. In this context, the initial phases of well drilling projects begin with the installation of the conductor casing, which can be carried out using different methods, including impact driving. This operation consists of three distinct stages: self-weight penetration, suction and hammering. As this is often an operation carried out in hostile environments, experimental analysis of drilling parameters becomes unfeasible, making numerical modeling of the problem a feasible and reliable alternative for controlling process variables.

Typically, problems in the mechanics of materials are addressed using the Finite Element Method (FEM). However, FEM faces challenges in handling large deformations, leading to significant mesh distortions and convergence issues [1]. To overcome these challenges, particle-based methods such as the Material Point Method (MPM) have been developed. Simulations of this nature are inherently complex due to the influence of multiple factors, including intrinsic problem parameters and numerical simulation variables. Proper calibration is essential,

considering the computational cost, to achieve solutions that closely match experimental results for the same problem.

In literature, it is common to encounter studies that analyze numerical parameters of simulations in various engineering problems, applied to their respective numerical methods. Examples of such studies using MPM include the work of Ceccato and Simonini [2], who simulated piezocone penetration tests (CPTu) and incorporated into their analyses the influence of material point specification in clayey soil. Another example is Martinelli and Galavi [3], who developed computational modeling of Cone Penetration Tests (CPT) in sandy soil, investigating the influence of several numerical parameters, including computational mesh refinement and numerical integration method. In this context, this work aims to understand how certain numerical parameters of MPM can influence soil behavior during the self-weight penetration phase of a conductor casing through the displacement achieved and the soil stress patterns. Such analysis will enhance our understanding of the process and potentially lead to an optimization of the problem, considering the associated computational costs.

2 Methodology

The installation process is known for its complexity and simulating it can be challenging due to the occurrence of large deformations. To tackle this, the ANURA 3D was used to model and simulate the conductor casing installation numerically. This software is designed for the numerical modeling and simulation of large deformations using the Material Point Method (MPM).

2.1 Material Point Method

The Material Point Method (MPM) was originally developed by Sulsky and Schreyer [4] to solve fast transient impact solid mechanisms problems [5]. It integrates the advantages of point-based and mesh-based methods. MPM uses an Eulerian-Lagrangian approach, where space is discretized into an Eulerian mesh and the modeled continuous body is discretized into material points that store the material properties. Fig. 1 shows the computational cycle of MPM. The material points transfer state variable values to the mesh nodes. The updated calculations at the nodes are then transferred back to the material points. At the end of each time step, the mesh is reset to its initial position, while the particles remain in their displaced positions, preventing excessive distortion of the elements. Information stored at the nodes is not permanent, thereby eliminating issues related to mesh distortion [6, 7, 8].

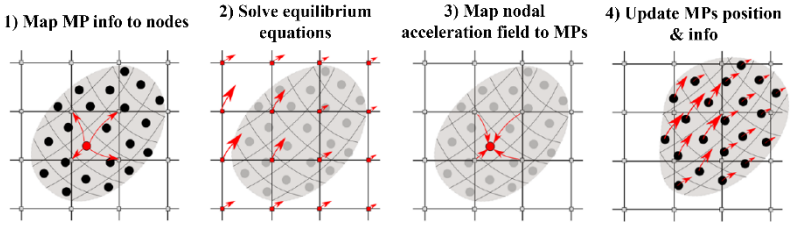

Figure 1. Illustration of the material point method [7].

2.1.1 Two phase single point formulation

An explicit dynamic two-phase formulation in MPM has been developed to consider soil and water interactions. It considers the generation and dissipation of pore water pressure during the structure installation process, accounting for dynamic waves in both water and solid phases [2, 9] in cohesive soils under saturated conditions, for example. The governing equations are mass conservation, momentum conservation and a constitutive model provide the solution of the system, described in equations 1 to 5. These equations solve for the accelerations of the pore liquid and soil skeleton as the primary unknown variables [3, 10].

$$\rho_L \boldsymbol{a}_L = \nabla \cdot (p_L \boldsymbol{I}) + \rho_L \boldsymbol{b} - \frac{n\mu_L}{\kappa_L}(\boldsymbol{v_L} - \boldsymbol{v_S}) \tag{1}$$

$$(1-n)\rho_S \boldsymbol{a} + n\rho_L \boldsymbol{a}_L = \boldsymbol{\nabla}\cdot(\boldsymbol{\sigma}' + p_L \boldsymbol{I}) + \rho_m \boldsymbol{b} \tag{2}$$

$$\frac{dn}{dt} = (1-n)(\nabla \cdot \boldsymbol{v_S}) \tag{3}$$

$$\dot{P_L} = \frac{K_L}{n}[(1-n)\nabla\cdot\boldsymbol{v}_S + n\nabla\cdot\mathbf{v}_L] \tag{4}$$

$$\dot{\boldsymbol{\sigma}}' = \boldsymbol{D}\dot{\boldsymbol{\varepsilon}}_S - \boldsymbol{\Omega}\boldsymbol{\sigma}' - \boldsymbol{\sigma}'\boldsymbol{\Omega} - \dot{\varepsilon_{v,S}}\boldsymbol{\sigma}.' \tag{5}$$

Where, n is the porosity; ρ_S and ρ_L and are the densities of the solid grains and liquid, respectively; ρ_m is the mixture density ($\rho_m = (1-n)\rho_S + n\rho_L$); $\boldsymbol{I}$ is the identity tensor; $\boldsymbol{v_S}$ and $\mathbf{v}_L$ are, respectively, the velocities of the solid and liquid phases; $\boldsymbol{\sigma}'$is the stress tensor; K_L is the bulk modulus of pure water, and $\boldsymbol{b}$ is the body force vector; $\boldsymbol{D}$ is the stiffness matrix; ; $\dot{\boldsymbol{\sigma}}'$ and $\dot{\boldsymbol{\varepsilon}}_S$ are, respectively, the stress rate and strain rate of the solid phase; $\boldsymbol{\Omega}$ is the rotation tensor; and $\varepsilon_{v,S}$ is the volumetric strain increment [11]. The discretized forms of mass conservation is in equations 6 and 7:

$$\bar{M}_{L,i}\boldsymbol{a}_{L,i} = \bar{f}^{ext}_{L,i} - \bar{f}^{int}_{L,i} + \bar{f}^{d}_{i} \tag{6}$$

$$\bar{M}_{S,i}\boldsymbol{a_{S,i}} + \bar{M}_{L,i}\boldsymbol{a}_{L,i} = \bar{f}^{ext}_{i} - \bar{f}^{int}_{i} \tag{7}$$

In which $\bar{M}_{S,i}$ $\bar{M}_{L,i}$, $\bar{f}^{ext}_{L,i}$, $\bar{f}^{int}_{L,i}$ and $\bar{f}^{d}$are the nodal values, respectively, for: the mass matrix of the solid and liquid phases; the external force vector, internal force vector, and drag force. These forces depend on shape function calculated to material point (MP) position, number of MP in the cell computational grid and gravitational force.

2.1.2 Rigid Body Algorithm

The MPM has been developed using an explicit solver and as result. Explicit schemes necessitate small enough time steps to capture wave propagation in the system and a stiff or less permeable material needs lower time steps [9]. In addition, the larger the elastic modulus, the lower critical the time step, it results in very high computational cost to simulate rigid structures. The critical time step does not depend on rigid body stiffness, so simulating rigid structures as a rigid body can decrease computational time, as there is no need to integrate stresses at rigid material points [10]. The stiffness of a steel conductor is very high compared to the stiffness of soil, so the conductor can be assumed to be a rigid body [9, 12, 10].

According to Ceccato et al. [10], this algorithm works as follows: first, momentum and velocity is mapped from particles nodes calculating rigid body acceleration (Eq. 8) and it is prescribed to all the nodes that belong to Eq. 9. The nodal velocity is computed according to Eq. 10. The rigid body algorithm is embedded into the contact framework, so it is verified if the contact algorithm is applied then the rigid body velocity is written to all corresponding MPs.

$$\boldsymbol{a}_{rb} = \frac{\left(m_{rb}\boldsymbol{g} + \boldsymbol{t}_{rb} - \sum_{\boldsymbol{i=1}}^{\boldsymbol{n_c}} \boldsymbol{f^i_{soil}}\right)}{m_{rb}} \tag{8}$$

$$\boldsymbol{a}^i_{rb} = \boldsymbol{a_{rb}}, \text{ for } 1 \le i \le \boldsymbol{n_{rb}} \tag{9}$$

$$\boldsymbol{v^i_{rb}} = \boldsymbol{v}^i_0 + \boldsymbol{a}^i_{rb}\Delta t, \text{ for } 1 \le i \le \boldsymbol{n_{rb}}, \tag{10}$$

where $\boldsymbol{g}$ is the gravitational force, $\boldsymbol{a}_{rb}$ and $\boldsymbol{m}_{rb}$ are the acceleration vector and total mass of rigid body, respectively, $\boldsymbol{t}_{rb}$ is the external load vector applied to the rigid body (equal to zero in this case), $\boldsymbol{n}_c$ is the number of nodes and $\boldsymbol{i}$ is the node relative index within the contact surface, respectively, $\boldsymbol{f^i_{soil}}$ is the force transmitted from soil to the structure at i-th contact node. Finally, $\boldsymbol{a}^i_{rb}$ and $\boldsymbol{v^i_{rb}}$ are the nodal acceleration and nodal velocity of the rigid body, respectively, Δt is the increment time and $\boldsymbol{v}^i_0$ is the velocity at beginning of each-time step.

2.1.3 Contact Algorithm

Contact is important to understand many engineering problems, including conductor-soil interaction. A contact happens when two deformable solids touch each other, however, it is easier in MPM due is background grid [8]. The advantage of this algorithm is that it automatically detects the contact surface, meaning there is no need to define any special elements at the interface between bodies [14, 10]. A frictional contact algorithm developed by Bardenhagen et al [15] with addiction of Al-Kafaji [14] for adhesive soils is used to modelling interaction between structure and soil [9]. The contact effect occurs due to the correction of the velocity difference between bodies A and B ($\boldsymbol{v}_{i,A}$ and $\boldsymbol{v}_{i,B}$) and the combined system velocity ($\boldsymbol{v}_{i,S}$), which are resolved by momentum equations at the node $\boldsymbol{i}$. Considering prescribed velocity of body A in instant $t + \Delta t$:

$$if \begin{cases} (v_{i,A}^{t+\Delta t} - v_{i,S}^{t+\Delta t}) \cdot n_i^t > 0, & approaching; \\ (v_{i,A}^{t+\Delta t} - v_{i,S}^{t+\Delta t}) \cdot n_i^t < 0, & separating\ , \end{cases} \tag{11}$$

where, n_i^t is the unit outward normal to body A at node i. Upon detecting the approach, the algorithm analyzes whether adhesion occurs between the bodies and obtains their corrected nodal velocities, including adhesion and friction terms. The corrected velocity of A, $\tilde{\boldsymbol{v}}_{i,A}$ can be obtained using Equation 12 [2, 10]:

$$\tilde{\boldsymbol{v}}_{i,A} = \boldsymbol{v}_{i,A} - \left[(\boldsymbol{v}_{i,A} - \boldsymbol{v}_{i,S}) \cdot \boldsymbol{n}_{i,A}\right]\boldsymbol{n}_{i,A} + \left[(v_{i,A} - \boldsymbol{v}_{i,S}) \cdot \boldsymbol{n}_{i,A}\right]\mu \boldsymbol{t_i} - \frac{aA_i \Delta t}{m_{i,A}}\boldsymbol{t_i}, \tag{12}$$

where, A_i is the surface area associated with node i and t_i is the tangential factor, μ is the friction coefficient and a is the adhesion factor.

2.2 Numerical Model of Conductor Casing Installation

Numerical simulation of conductor casing installation has been developed in a 2D-axisymmetric MPM. A default computational model was established to conduct analysis of numerical parameters. The Fig. 2 below shows the geometry employed, as well as its features such as dimensions, mesh refinement and constraints. This geometry uses 3-noded triangular elements, and a mixed integration approach, which utilizes material points (MP) and Gauss points, was employed to calculate the internal forces. The advantage of the mixed integration scheme is its mitigation of cell-crossing instabilities and stress oscillations [10, 13].

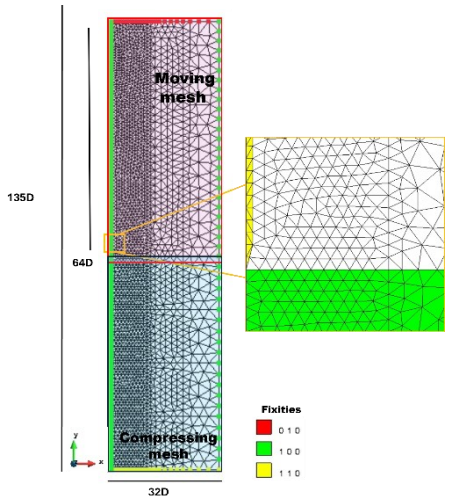

Figure 2. Geometry, mesh and fixities of 2D-axisymmetric model in MPM (Authors, 2024).

The penetration resistance of the conductor arises from a combination of clay adhesion on both the inside and outside surfaces and the end bearing resistance across the cross-sectional area, or the entire area if plugging occurs [16]. Thus, this may imply some operational simplifications that can be made to simulate problems of this magnitude. Based on this assumption, the present modeling considers the conductor casing as a massive structure, in order to simplify the problem under analysis, considering the external radius of the conductor casing as a minor

element in the domain.

The geometry and mesh of the computational model illustrated in Fig. 2 show a conductor casing with a diameter of D = 0.91m (36in). The length of the casing (64Dm), as well as the height and bottom of the domain, vary with D. This geometry utilizes an unstructured mesh, with increased refinement near the casing to enhance result accuracy. The domain shown in Fig. 2 includes 6 material points per element in the soil (green region) and 1 material point per element in the conductor casing (yellow region). The total number of material points is 6773. Additionally, this geometry comprises 4778 elements and 2504 nodes. The casing is above ground, and its installation occurs through self-weight penetration into the soil. A moving mesh procedure [14] is applied in the domain to ensure that soil-conductor casing elements maintain consistent shapes throughout the simulation, as the contact nodes on the conductor casing and soil always remain at the same coordinates. This approach helps reduce oscillations in contact forces [9, 3, 10,13]. The simulations were performed on a computer with the following specifications: Intel Core i5-9600K (@3.70 GHz), 16 GB of RAM, and Windows 11 (64-bit).

2.3 Properties

In order to model this work, the data was obtained from CPTu tests provided by the company. Based on the analysis of the data it was established that the Mohr-Coulomb constitutive model would be suitable for modeling the response of the cohesive undrained soil considered in this work. Some of these parameters should be mentioned, such as the initial porosity of 0.58, density of 1475.40 kg/m³, Bulk Modulus of $2.15(10^{4})$, dynamic viscosity of $1.57(10^{-6})$ Kpa.s and the K0 value of 0.96. Regarding the Mohr-Coulomb criteria parameters, notable values include a Poisson's ratio of 0.49, an effective elasticity modulus of 17896.06 kPa, and effective cohesion and friction angle of 36.29 kPa and 0.43 rad, respectively. Additionally, during the modeling stage of the soil-conductor contact, the adhesion factor of 4.64 kPa stands out.

3 Results

To better understand the problem under investigation, several associated numerical parameters need further examination to validate the model. Therefore, to explore the impact of these parameters on results such as depth reached and stress behavior, some results will be presented.

The first part of the analysis consisted of varying the material point (MP) specifications per element in the soil region and fixing other numerical parameters. The gain in depth decreases over time due to increasing soil resistance, causing the curve to stabilize. Figure 3 illustrates how these variations in material points influence the achieved depth, aiming to determine an optimal value at a specific point. The curve corresponding to 3MP stabilizes around 25m, while 6MP and 12MP curves stand around 21m.

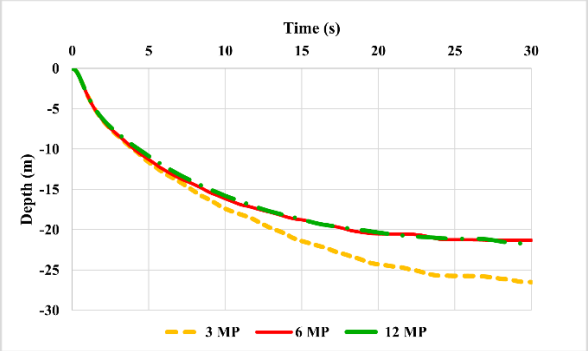

Figure 3. Comparison of the depth reached with different material points in the soil (Authors, 2024).

As shown, the curves for 6 material points and 12 material points behave very similarly but differ in computational cost. Table 1 presents the computational costs associated with the models, indicating that as the number of material points increases, the computational effort also increases. Therefore, for further analysis, the model with 6 material points in the soil is preferred, as it offers a lower computational cost while still providing

effective results for the required analysis.

Table 1. File Size and Simulation time

MP Specification	Simulation Time	Size
3 MP	14:27 hrs	99.7 GB
6 MP	27:22 hrs	191 GB
12 MP	58:04 hrs	375 GB

Figure 4 presents the vertical effective stress distribution in soil. When examining the stresses near the conductor casing, there is an expected increase in stresses at the tip region as shown in Fig. 4. Although the results appear similar, the dissipation of these stresses is more precise in the cases with 6 and 12 material points. Increasing the material point specification does not result in significant improvement to justify the increase in computational cost.

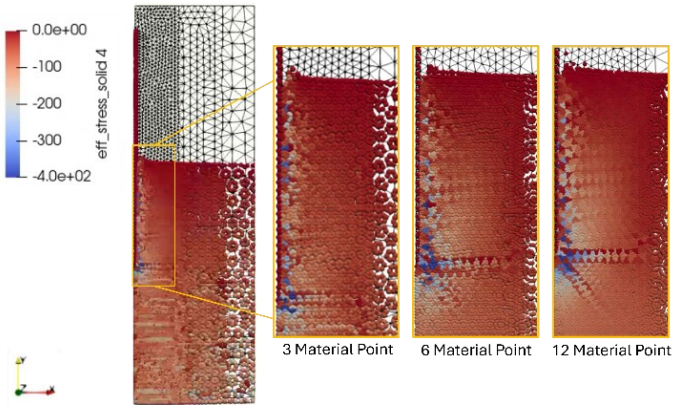

Figure 4. Comparison of the vertical effective stress (kPa) with different material points in the soil

Another analysis to consider is the evaluation of the time step implementation. Figure 5 illustrates four different time increments analyzed for this problem. Decreasing the time steps improves result accuracy but also extends the computational time needed for the simulation. However, the figure shows that, for this particular problem, reducing the time step does not significantly enhance the results.

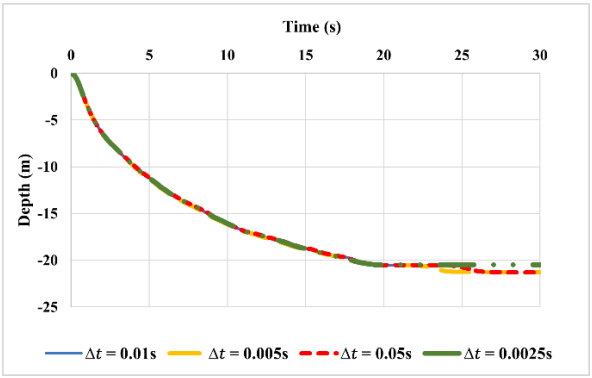

Figure 5. Comparison of the depth reached with different time step (Authors, 2024).

Table 2. File Size and Simulation time

Time Step	Simulation Time	Size
0.0025s	36:23 hrs	380 GB
0.005s	27:22 hrs	191 GB
0.01s	12:45 hrs	95 GB
0.05s	06:25 hrs	19 GB

In terms of computational cost, there is a significant difference between the analyses performed. As expected,

shorter time steps lead to higher computational costs and greater memory consumption. In this context, choosing a larger time step appears to optimize the solution, allowing for greater progress.

4 Conclusions

The MPM proved to be a promising approach for numerical modeling of conductor casing driving, even if simplification strategies are considered, such as assuming an isotropic and uniform soil layer and using a 2D-axisymmetric procedure. Analysis of numerical parameters helped to understand computational behavior in terms of simulation time and file size. In this case, increasing the material point specification improved results for vertical displacement and tension distribution up to 6MP. When adopting 12MP, these results did not show any significant difference, only increasing computational costs. Similarly, decreasing the time increment did not reveal any significant differences even though smaller time increments lead to higher accuracy of the result. For future work, we aim to study the influence of mesh refinement and contact numerical parameters on the results, including other stages of conductor casing driving such as suction and hammering beside self-weight installation.

Authorship statement. The authors hereby confirm that they are the sole liable persons responsible for the authorship of this work, and that all material that has been herein included as part of the present paper is either the property (and authorship) of the authors, or has the permission of the owners to be included here.

References

[1] Nazem, M., Sheng, D. & Carter, J. P. Integração da tensão e refinamento da malha para grandes deformações em geomecânica. International Journal for Numerical Methods in Engineering, 65, pp,1002-1027, (2006).
[2] Ceccato, Francesca; Simonini, Paolo. Numerical study of partially drained penetration and pore pressure dissipation in piezocone test. Acta Geotechnica, v. 12, p. 195-209, 2017.
[3] Martinelli, M.& Galavi, V. Investigation of the material point method in the simulation of cone penetration tests in dry sand. Computers and Geotechnics, 130:103923, 2021.
[4] Sulsky, Deborah; Chen, Zhen; Schreyer, Howard L. A particle method for history-dependent materials. Computer methods in applied mechanics and engineering, v. 118, n. 1-2, p. 179-196, 1994.
[5] Nguyen, Vinh Phu; De Vaucorbeil, Alban; Bordas, Stephane. The material point method. Cham: Springer International Publishing, 2023.
[6] Yerro, Alba; Girardi, Veronica; Martinelli, Mario; Ceccato, Francesca. Modelling unsaturated soils with the Material Point Method. A discussion of the state-of-the-art. Geomechanics for Energy and the Environment, v. 32, p. 100343, 2022.
[7] Yost, Kaleigh M., Yerro, Alba; Green, Russell A.; Martin, Eileen; Cooper, Jon. MPM modeling of cone penetrometer testing for multiple thin-layer effects in complex soil stratigraphy. Journal of Geotechnical and Geoenvironmental Engineering 148.2 (2022): 04021189.
[8] Zheng, Xiangcou et al. Material point method simulation of hydro-mechanical behaviour in two-phase porous geomaterials: A state-of-the-art review. Journal of Rock Mechanics and Geotechnical Engineering, v. 16, n. 6, p. 2341-2350, 2024.
[9] Galavi, V. et al. Numerical simulation of impact driven offshore monopiles using the material point method. Proceedings of the XVII ECSMGE-2019, 2019.
[10] Ceccato, Francesca; Fern, James; Martinelli, Mario, et al. Anura 3D MPM Software, Scientific Manual, 2022.
[11] Martinelli, Mario & Galavi, Vahid. An Explicit coupled MPM Formulation to Simulate Penetration Problems in Soils Using Quadrilateral Elements. Computers and Geotechnics, v. 145, p. 104-697, 2022.
[12] Martinelli, Mario & Alderlieste, Etienne & Luger, Dirk & Galavi, Vahid. Numerical Simulation of the Installation of Suction Buckets Using MPM. (2020).
[13] Yost, Kaleigh M.; Martinelli, Mario; Yerro, Alba; Green, Russell A.; de Lange, Dirk A. Addressing Complexities in MPM Modeling of Calibration Chamber Cone Penetrometer Test in Homogenous and Highly Interlayered Soils. Computers and Geotechnics, v. 158, p. 105-378, 2023.
[14] Kafaji, Issam. Formulation of a Dynamic Material Point Method (MPM) for Geomechanical Problems. Dissertation, Universität Stuttgart. 2013.
[15] Bardenhagen, S.G., Guilkey, J.E., Roessig, K.M., Brackbill, J.U., Witzel, W.M., Foster, J.C. An improved contact algorithm for the material point method and application to stress propagation in granular material, C. - Comput. Model. Eng. Sci. 2 (2001) 509–522.
[16] Leach, Colin, and Tony Bamford. "Use of Drilled-in Casing in Slim Deepwater Exploration Wells." Paper presented at the SPE/IADC Drilling Conference, Amsterdam, Netherlands, February 2005.